f_{max} Enhancement of HBTs Using New Self-Aligned Emitter-Base Metallization Technique

Kwangsik Choi, Daekyu Yu, Kyungho Lee, and Bumman Kim

Department of Electrical and Computer Engineering
Pohang University of Science and Technology
E-mail : torisis@postech.ac.kr

Abstract : A new self-aligned emitter-base metallization (SAEBM) technique is developed for high speed heterojunction bipolar transistors (HBTs). After the mesa etch for base layer using photo resist mask, the base and emitter metals evaporated simultaneously. The process reduces the emitter-base gap and base gap resistance (R_{GAP}). The InP/InGaAs/InP double heterojunction bipolar transistors (DHBTs) fabricated using the technique have smaller base resistance, from 16.48 Ω to 4.62 Ω by comparing the DHBT with conventional self-aligned base metallization (SABM) process. Due to the reduced R_{GAP}, the maximum oscillation frequency (f_{max}) is improved from 205 GHz to 295 GHz and the cutoff frequency (f_T) is maintained similarly.

1. Introduction

The operation frequency of transistor is pushed steadily into higher frequencies due to the demand for high speed circuits. To achieve the high cutoff frequency (f_T) and the maximum oscillation frequency (f_{max}), which are the figures of merit for high speed performances, the HBT design must: achieve low base and collector transit times for high f_T, balance between collector transit time, breakdown voltage and base-collector capacitance (C_{CB}), minimize the base resistance (R_B), minimize the extrinsic C_{CB}, and minimize the emitter contact resistance (R_E). Especially C_{CB} and R_B are important factors for the high f_{max} since $f_{max} \cong (f_T/8\pi R_B C_{CB})^{1/2}$. Many research works have been devoted to reduce the C_{CB} and R_B. To reduce the C_{CB}, ion implantation technique and undercut technique are widely used [1][2]. Another solution to reduce C_{CB} is scaling device laterally [3]. To reduce R_B, base layer is thick and doped as high as possible. But the doping concentration is limited by epi growth technology, 8E19 cm^{-3} for p-type InGaAs, and the thickness can not be thick limited by base transit time.

R_B is composed of intrinsic base resistance (R_{BI}), base contact resistance (R_{CONT}), and base gap resistance (R_{GAP}). R_{BI} can be controlled by vertical and lateral scaling. And R_{CONT} is minimized by optimized metal composition, Pt for p-type InGaAs, but cannot be scaled. R_{GAP} is not a scalable parameter and emitter-base gap should be minimized for small R_{GAP}.

In this paper, new self-aligned emitter-base metallization (SAEBM) technique is proposed to reduce R_{GAP} by reducing the gap. And we could significantly improve f_{max} using the process.

2. Device Structures and Fabrications

The epitaxial layer of the fabricated DHBTs is grown by IntelliEPI using Solid Source Molecular Beam Epitaxy (SSMBE) on an Fe-doped semi-insulating (100) InP substrate. The base layer is highly doped to 8E19 cm^{-3} to obtain a low base sheet resistance. To achieve a high β and reduce base transit time, the base layer is linearly compositional graded from x = 0.46 to 0.53 toward collector, and thin, 250 Å. To remove the carrier blocking effect due to the conduction band discontinuity between InGaAs (base) and InP (collector), the linearly compositional graded $In_{(x)}Ga_{(y)}Al_{(1-x-y)}As$ layer is employed at the collector. Additionally, to compensate the reverse electric field induced by the graded layer, delta-doped InP layer is introduced within collector layers [4]. Sub-collector layers are designed suitable for the undercut process explained in reference [5]. The whole layer structure is shown in Table 1.

Fig.1.(a) shows the conventional processes using SABM for InP-based HBTs or DHBTs. In the process, the emitter mesa is etched laterally during emitter mesa etching, and the space (S_{BE}) between emitter mesa and base metal is widened. The widened S_{BE} increases the R_{GAP} because the resistance is proportional to S_{BE}. Thin emitter can be a solution to avoid the lateral etching of emitter mesa, and sidewall processes are also employed to prevent the connection between emitter metal and base metal [6].

In our new SAEBM technique, the emitter mesa is etched using the PR mask of emitter patterns at first. After removing PR pattern, metallization process is followed for both emitter and base contacts simultaneously with Pt/Ti/Pt/Au. When emitter mesa is formed in the $[01\bar{1}]$

crystal direction, the mesa has a shape of trapezoid. Because the thickness of emitter and emitter cap layer is high and the shape of emitter mesa is a trapezoid, the emitter and base metal contacts are formed safely without connection between emitter and base metals. The schematic of new process flows is depicted in Fig.1.(b)

When the conventional SABM process is used, S_{BE} is about 250 nm as shown in Fig. 2.(a). If the SAEBM process is used, S_{BE} of 80nm is expected from Fig. 2.(a). Fig. 2.(b) shows a test pattern after SAEBM process and S_{BE} is confirmed to be reduced below 100 nm, about 80 nm. Because the emitter metal is deposited after emitter mesa etching at the SAEBM, the lateral etching of emitter mesa does not affect the space between emitter mesa and base contact metal. This considerable reduction of S_{BE} is the advantage of SAEBM technique. Besides, the SAEBM process is simpler than SABM process.

Two types of InP/InGaAs/InP DHBTs are fabricated using conventional SABM technique, called DHBT-C, and new SAEBM technique, called DHBT-N with the same mask after base contact metallization. The emitter metal width is 0.8 μm, effectively 0.5 μm, for both DHBTs. The collector undercut process is carried out after base and collector mesa formation using the method suggested in the reference [5]. The comprehensive process sequence can be found in our previous work [7].

3. Results and Discussions

Normally the emitter metal is composed of Ti/Pt/Au for high doped n-type InGaAs emitter cap layer. The composition of emitter metal is changed to base metal, because the base resistance is a critical factor for high speed performance. Nevertheless, the specific contact resistivity of emitter layer, measured using transmission line measurement (TLM), is 1.8×10^{-8} Ω•cm^2 for DHBT-N, which is quite acceptable. The sheet resistance ($R_{SH,B}$) and specific contact resistivity ($\rho_{\sigma B}$) of base layer is 790 Ω/□ & 2.4×10^{-7} Ω•cm^2 for both DHBTs. The transfer length, L_T, expressed as $(\rho_{\sigma B}/R_{SH,B})^{1/2}$ is 0.4 μm and the base contact resistance is maintained low.

Small signal model parameters, listed in Table. 2, are extracted to analyze the base resistances of DHBTs with 0.5 × 6 μm^2 emitter geometry, at maximum f_{max} bias point. Most of extracted parameters are identical for the two devices except R_{BX}, 28.11 Ω and 15.10 Ω, respectively. R_B

Layer Description	Composition	Conc. [cm^{-3}]	Thickness [Å]
Emitter Cap	$In_{0.53}Ga_{0.47}As$	3E19 n+	1000
	$In_{(x)}Ga_{(y)}Al_{(1-x-y)}As$	3E19 n+	200
	InP	1E19 n+	900
Emitter	InP	7E17 n	700
Space	$In_{0.46}Ga_{0.54}As$	i	20
Base	$In_{(x)}Ga_{(1-x)}As$	8E19 p+	250
Collector	$In_{0.53}Ga_{0.47}As$	2E16 n	200
	$In_{(x)}Ga_{(y)}Al_{(1-x-y)}As$	2E16 n	300
	InP	1E18 n	30
	InP	2E16 n	1000
Sub Collector	InP	1E19 n+	200
	$In_{0.53}Ga_{0.47}As$	3E19 n+	3000
	InP	1E19 n+	100
	$In_{0.53}Ga_{0.47}As$	3E19 n+	3000
Substrate	Fe-doped Semi-insulated InP		

Table 1. **Epitaxial layer structure**

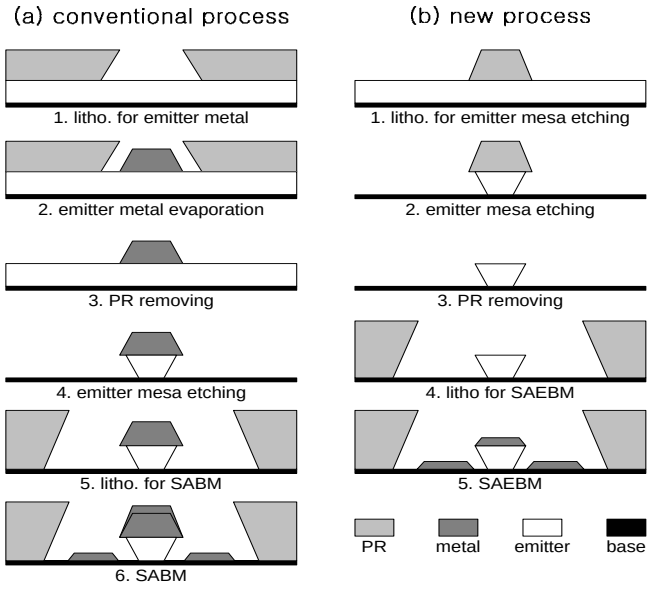

Fig. 1. **Process flow : (a) conventional process using SABM, (b) new process using SAEBM.**

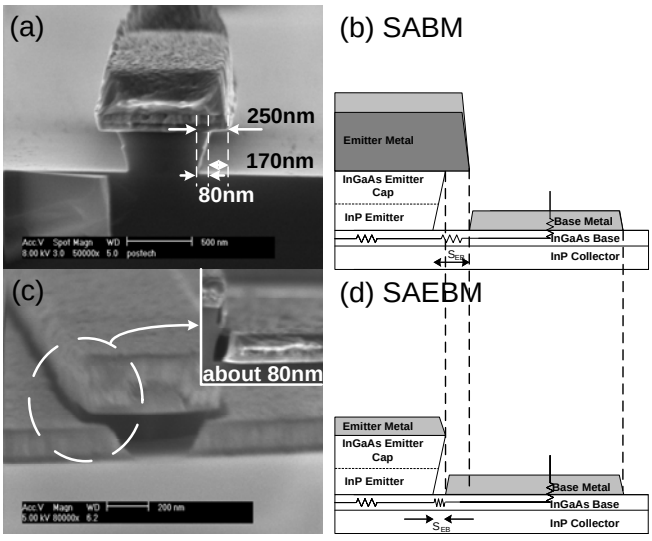

Fig. 2. **(a) SEM picture after emitter mesa etching using conventional wet etching, (b) Schematic of SABM process, (c) SEM picture after SAEBM process, (d) Schematic of SAEBM process**

is a sum of R_{BI}, R_{CONT}, and R_{GAP} and can be calculated geometrically by

$$R_B = R_{BI} + R_{CONT} + R_{GAP} \quad (1)$$

$$R_{BI} = \frac{1}{12} \cdot R_{SH,B} \cdot \frac{W_E}{L_E} \quad (2)$$

$$R_{GAP} = \frac{1}{2} \cdot R_{SH,B} \cdot \frac{S_{BE}}{L_E} \quad (3)$$

$$R_{CONT} = \frac{1}{2} \cdot \frac{\sqrt{R_{SH,B} \cdot \rho_{\sigma B}}}{L_E} \cdot \coth\left(W_B \cdot \sqrt{\frac{R_{SH,B}}{\rho_{\sigma B}}} \right) \quad (4)$$

The difference of R_{BX} between DHBT-C and DHBT-N is the result of reduced S_{BE}, that is, reduction of R_{GAP}. Since S_{BE} is reduced from 250 nm to 80 nm from the SEM picture, R_{GAP} is reduced from 16.48 Ω to 4.62 Ω by using equation (3), about 72 % reduction of R_{GAP} at 0.5 × 6 μm^2 emitter geometry. This reduction is about 39% of total base resistance of DHBT-C. Table. 3 lists the extracted and calculated base resistances of both DHBTs.

	R_E	R_{BI}	R_{BX}	g_m	r_π	C_π	C_{CBI}	C_{CBX}
DHBT_C	8.49	4.79	28.11	0.45	67.1	0.19	2.55	5.42
DHBT_N	7.27	5.11	15.10	0.42	62.2	0.17	2.50	5.38

Table 2. **Extracted small-signal parameters**

	extracted para. [Ω]		calculated para. [Ω]		
	R_{BI}	R_{BX}	R_{BI_cal}	R_{BX_cal}	
				R_{CONT}	R_{GAP}
DHBT-C	4.79	**28.11**	5.49	11.49	**16.48**
DHBT-N	5.11	**15.10**	5.49	11.49	**4.62**

Table 3. **De-composition of base resistance**

The measured common emitter I-V curve of the fabricated DHBTs with 0.5 × 6 μm^2 emitter area is depicted in Fig. 3. The common-emitter dc current gain (β) of DHBT-C and DHBT-N is about 30 and 25 respectively. The breakdown voltage of two devices at an open base, BV_{CEO}, is similar as 6.2 V at 100 μA collector current.

The difference of β between DHBT-C and DHBT-N can be explained by analysis of base current, composed of surface recombination current (J_{SURF}), contact recombination current (J_{CONT}), bulk recombination current (J_{BULK}), space-charge recombination current (J_{SCR}), and back-injected hole current (J_{BP}). With the periphery dependency of J_{SURF} and J_{CONT} and the area dependency of the others, Jc/β is expressed by

$$\frac{J_c}{\beta} = J_{BULK} + J_{SCR} + J_{BP} + 2(J_{SURF} + J_{CONT}) \times \left(\frac{1}{W_E} + \frac{1}{L_E} \right) \quad (5)$$

where J_c is collector current density. Jc/β is measured as a function of $(1/W_E + 1/L_E)$ and depicted in Fig. 4. Through the linear fitting, $J_{SURF} + J_{CONT}$ of DHBT-N is higher than DHBT-C at both $J_C = 1 \times 10^4$ A/cm^2 and $J_C = 5 \times 10^4$ A/cm^2.

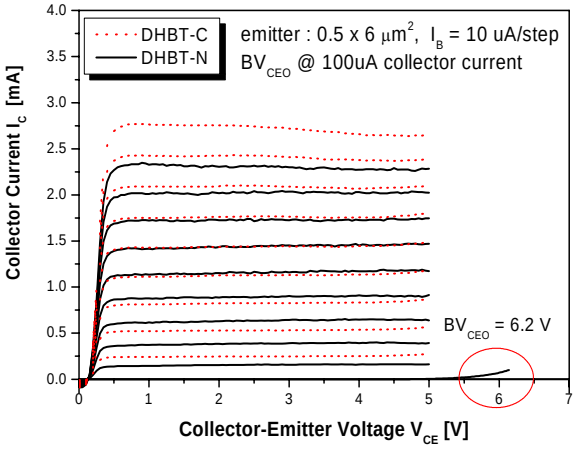

Fig. 3. **Common emitter DC I_C-V_{CE} characteristics.**

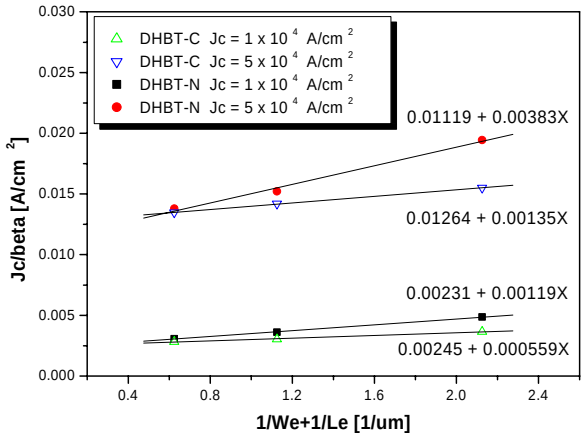

Fig. 4. **Jc/β versus $(1/W_e + 1/L_e)$ characteristics.**

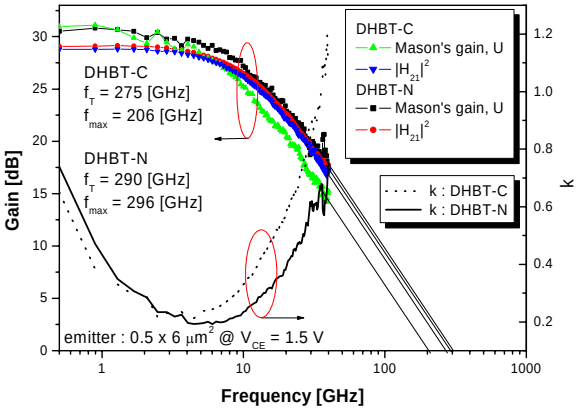

Fig. 5. **Frequency dependences of Mason's gain U, $|H_{21}|^2$, and stability factor (k) for fabricated DHBTs.**

Since the surface recombination current can be neglected for low surface recombination velocity of p-type InGaAs, this increased periphery dependent currents are caused by increased base contact recombination current due to widened base metal width of DHBT-N. Therefore DHBT-N has smaller ß than DHBT-C.

Microwave performances are characterized by on-wafer S-parameter measurements from 0.5 to 40 GHz using a HP8510C vector network analyzer. Fig. 5 shows the frequency dependences of current gain $|H_{21}|^2$, Mason's unilateral gain, and stability factor (k) of both DHBTs at the same bias point. DHBT-N has lower k than DHBT-C dud to the reduced base resistance. The f_T and f_{max} are obtained assuming a –20 dB/decade frequency dependence of the current gain and Mason's unilateral gain, respectively. For DHBT-C, f_T = 275 GHz and f_{max} = 206 GHz are obtained at J_C = 3.63 kA/cm^2 and V_{CE} = 1.5 V. For DHBT-N, f_T = 290 GHz and f_{max} = 296 GHz are obtained at J_C = 3.85 kA/cm^2 and V_{CE} = 1.5 V. Since the base resistance does not affect the transit time, f_Ts of the two DHBTs are similar. But the f_{max} of DHBT-N is improved about 90 GHz by using the SAEBM technique. This RF performance results show that the SAEBM is very effective technique to enhance f_{max} clearly.

4. Conclusions

The new but simple SAEBM technique has developed to improve the high speed performance, especially f_{max}, of HBTs. Using SAEBM technique for InP-based DHBTs, R_{GAP} is redeced from 16.48 Ω to 4.62 Ω and f_{max} is improved about 90 GHz without trade-off degrading f_T. High frequency performances of f_T = 290 GHz and f_{max} = 296 GHz are obtained for a 0.5 × 6 μm^2 DHBT-N with BV_{CEO} = 6.2 V. The RF performance results demonstrate the effectiveness of the new SAEBM technique for enhanced performance. Further improvements of f_{max} and f_T are expected by lateral scaling in the geometrical layout and parasitic reductions. Besides, if the emitter mesa etching is controlled precisely, nano-scale HBTs can be fabricated using SAEBM technique without e-beam lithography technology.

References

[1] K. Lee, *et. al,* "New Collector Undercut Technique Using a SiN Sidewall for Low Base Contact Resistance in InP/InGaAs SHBTs," *IEEE Trans. Electron Devices*, vol. 49, No. 6, pp. 1079-1082, 2002.

[2] D. Yu, *et. al*, "Realization of High-Speed InP SHBTs using Novel but Simple Techniques for Parasitic Reduction," *IEEE Indium Phosphide and Related Materials (IPRM)*, pp. 753-756, 2004.

[3] M. J. W. Rodwell, *et. al*, "Submicron Scaling of HBTs," *IEEE Trans. Electron Devices*, vol. 48, No. 11, pp. 2606-2624, 2001.

[4] T. R. Block, *et. al*, "Molecular beam epitaxy growth and characterization of InGaAlAs-collector heterojunction bipolar transistors with 140 GHz f_{max} and 20 V breakdown," *J. Vac. Sci. Technol.*, B 14(3), pp. 2221-2224, 1996.

[5] Y. Jeong, *et. al*, "f_{max} enhancement in InP-based DHBTs using a new lateral reverse-etching technique," *Indium Phosphide and Related Materials (IPRM)*, pp. 22-25, 2003.

[6] Z. Grifith, *et. al,* "Wide Bandwidth InP DHBT Technology Utilizing Dielectric Sidewall Spacers," *IEEE. IPRM,* pp. 667-670, 2004.

[7] D. Yu, *et. al*, "Ultra High-Speed InP/InGaAs SHBTs with f_{max} of 478 GHz," *IEEE Electron Device Letters*, Vol. 24, No. 6, pp. 384-386, 2003.